

Original Research

Characteristics and Causes of Seasonal Changes in Dissolved Inorganic Carbon and Its Isotopes in a Typical Karst Underground River Basin

Qingqing Xiong¹, Dijin Mu¹, Hao Wang¹, Zhongli Wu¹, Shizhen Xiao^{1, 2*}

¹School of Karst Science, Guizhou Normal University/State Engineering Technology Institute for Karst Desertification Control, Guiyang 550001, Guizhou, China

²The College of Resources and Environmental Engineering, Guizhou University, Guiyang 550025, Guizhou, China

Received: 19 March 2024

Accepted: 23 August 2024

Abstract

Dissolved inorganic carbon isotopes ($\delta^{13}\text{C}_{\text{DIC}}$) are an important means to trace the different sources and influence characteristics of dissolved inorganic carbon (DIC). In this paper, 11 sampling sites were set up in the Huanghou underground river basin, a typical karst watershed for field sampling in the dry season (February) and wet season (May) in 2022, respectively. The aim was to investigate the seasonal characteristics of rivers DIC and $\delta^{13}\text{C}_{\text{DIC}}$. The results showed that the various water chemistry parameters (anions, cations, pCO_2 , DIC, and $\delta^{13}\text{C}_{\text{DIC}}$) in the basin showed significant seasonal variations in the dry and rainy seasons, with Ca^{2+} as the dominant cation, HCO_3^- as the dominant anion, and HCO_3^- -Ca as the chemical type of the water in the basin; nitric and sulfuric acids in the watershed waters are involved in the weathering of carbonate rocks. The dry season variation of DIC in this basin ranged from $213.57 \text{ mg}\cdot\text{L}^{-1}$ to $231.88 \text{ mg}\cdot\text{L}^{-1}$ with a mean value of $221.34 \text{ mg}\cdot\text{L}^{-1}$, and the rainy season variation ranged from $189.16 \text{ mg}\cdot\text{L}^{-1}$ to $237.98 \text{ mg}\cdot\text{L}^{-1}$ with a mean value of $206.36 \text{ mg}\cdot\text{L}^{-1}$; whereas the mean value of $\delta^{13}\text{C}_{\text{DIC}}$ was -4.91% in the dry season and -9.97% in the rainy season, which showed a positive pattern in the dry season and a negative pattern in the rainy season. The source of DIC in the study area is mainly attributed to dissolution of carbonate rocks and soil CO_2 ; the percentage of dissolved carbonate rocks in the dry season DIC ranged from 86.52% to 67.61% , and the percentage of soil CO_2 ranged from 13.48% to 32.39% , while the percentage of dissolved carbonate rocks in the wet season DIC ranged from 59.57% to 53.83% , and the percentage of soil CO_2 ranged from 40.43% to 46.17% . The chemical properties of waters in the basin are less affected by human activities and show a strong natural river character.

Keywords: hydrochemistry, dissolved inorganic carbon (DIC), dissolved inorganic carbon isotopes ($\delta^{13}\text{CDIC}$), underground river basin

Introduction

From 1990-2020, global carbon emissions show a change from 22727.88 to 35962.87 million tons, CO_2

* e-mail: 349871690@qq.com

gas in the global context shows a continuous increase in the emission state (<https://www.shujujidi.com/shehui/1.html>), and rivers as the surface weathering of the formation of dissolved substances from the land into the ocean, connecting the land and the river in the water-gas interface and thus achieving an important role in carbon cycling. Rivers play an important role in biogeochemical cycling [1-2]. Previous studies have shown that 60 percent of the approximately 1 PgC input from land to the oceans each year is in the form of dissolved inorganic carbon (DIC) [3]. Consequently, the existence state and source of carbon in rivers and the influencing factors of the temporal and spatial changes of dissolved inorganic carbon in rivers with seasons are worthy of in-depth study.

Since the stable isotopes of the contributing sources of dissolved inorganic carbon in rivers vary, the isotope tracing of DIC ($\delta^{13}\text{C}_{\text{DIC}}$) is a good reflection of the geochemical behavior and cycling characteristics of carbon in rivers and is an important indicator for identifying processes such as karst action in rivers [4-6]. Huang et al. used $\delta^{13}\text{C}_{\text{DIC}}$ to trace the source of carbon in karst groundwater [7], Zhao et al. used the magnitude of carbon isotope values to indicate the coverage of bare rock, soil, and vegetation in karst areas, which in turn facilitates the mastery of the potential changes in karst environments [8], and Zhao Y et al. calculated the contribution of the source of DIC to the groundwater in the Huixian Wetland based on inorganic carbon and its isotopes, which also reveals the source of DIC in the wetland while helping to understand the process of karst weathering. The weathering process also revealed the biogeochemical processes that affect the changes in its water quality and $\delta^{13}\text{C}_{\text{DIC}}$ values [9]. However, the composition of water chemistry in rivers in karst areas with a large distribution of karst environments is largely influenced by the weathering of carbonate rocks, and HCO_3^- showing high concentration values is one of the distinctive features of karst groundwater [10]. Previous research has shown that the weathering process of rocks presents regional variations with the infiltration of different factors such as rock type, climatic characteristics, biological respiration, plant photosynthesis, and human activities [11-12], which will also show variability under the influence of different anthropogenic acids [13]. Previous studies on riverine DIC in karst areas have mostly explored its sources and geochemical processes, while less consideration has been given to the biochemical processes of riverine DIC combined with quantitative studies.

The Huanghou underground river basin is the largest underground river system among the three underground river systems in the southern part of Dushan County, Guizhou Province, China, with a total length of 56 km from the upstream to the downstream [14], and the formation and development of this underground water system is closely related to the hydrological, geological, geomorphological, and meteorological conditions of the area and influences the evolution of the whole basin

and the geomorphological effects of karst landforms. At the same time, its well-developed underground water system can provide sufficient water resources for the production and life of the local community. Karst areas are highly susceptible to pollution due to the uniqueness of their groundwater systems [15], and at the same time, the increasing domestic sewage and tourism activities may expose the watersheds to human impacts to a certain extent as the watersheds flow through the towns' main streets, agricultural areas, and scenic spots. Therefore, the changes in water chemistry, DIC, and its isotopes in the watershed through two seasonal temporal variations were analyzed to explore the spatial and temporal distribution pattern of DIC, and its isotopes in the watershed, to further understand the biogeochemical characteristics of the underground river basin in the Huanghou area, and to make quantitative estimates in order to provide realistic support for the process of cycling carbon in the rivers of the karst region and the control of groundwater in the region.

Materials and Methods

Overview of the Study Area

The Huanghou underground river basin is located in the range of longitude 107°24'30"-107°45'00"E, latitude 25°10'00"-25°26'00"N, and the basin extends three counties, Dushan, Nandan, and Libo, with a total area of about 460 km². The soluble carbonate rock layers in the southern part of Dushan County are widely distributed, accounting for 86% of the whole area, and the strong permeability of the rock layers and the karst valleys and troughs interspersed throughout the area make the underground river in the area very developed, but the surface water resources are extremely scarce [13-14]. The Huanghou underground river basin, as a mid-subtropical karst catchment area, is located between the Guizhou Plateau and the Guangxi Basin, with an average precipitation of about 1425 mm per year, of which 78.1% is concentrated in the rainy season from May to October, and the average annual temperature is about 15°C. The Lashangdong groundwater provides an important source of drinking water for the villages in the surrounding area. The basin crosses the meridional tectonic belt, latitudinal tectonic belt, and New Huaxia tectonic belt, so the control of the underground river system by the joint deformation network is also more complicated, and the exposed lithology is mostly the Carboniferous carbonate rock and a small part of it is covered by the Permian sand shale. Due to the wide distribution of carbonate rocks and the existence of river intervals, the development of karst in this area is complicated, and it is one of the most developed karst areas in China [16].

Sample Collection

After the field visit, 11 sampling points were set up from upstream to downstream in the Huanghou underground river basin (Fig. 1), including surface water S1~S5 and groundwater G1~G6. Field samples were collected from the 11 sampling points (Table 1) in February and May 2022, respectively. Two 60 ml HDPE bottles and a 15 ml centrifuge tube were prepared for river water sample collection. The water samples were filtered through a 0.45 μm Millipore membrane using a syringe in the field and then packed into wet-washed 60 ml HDPE bottles and stored in sealed containers for anion and cation identification, in which the cation samples were acidified with ultra-pure HNO_3 dropwise to $\text{pH} < 2$ and stored in sealed containers. The water samples were filtered with a 0.22 μm filter membrane and put into 15 ml centrifuge tubes with lubricated lids, covered with HgCl_2 solution (2 drops), and sealed with parafilm to avoid isotope fractionation in the water samples for the determination of $\delta^{13}\text{C}_{\text{DIC}}$. All the collected water samples were kept in an insulated box under refrigeration and brought back to the laboratory for determination.

Measurement and Calculation Methods

Measurement Methods

The main methods of determination were a

combination of on-site measurement by the instruments, on-site titration, and sending back to the laboratory for determination. At the sampling site, the French PONSELODEON (ODEON Multy8320) portable multi-parameter water quality detector was used to determine the water temperature (T), pH, dissolved oxygen (DO), and electrical conductivity (EC) in the water column, and its measurement accuracy was 0.1°C, 0.01, 0.01 $\text{mg}\cdot\text{L}^{-1}$, and 1 $\mu\text{S}\cdot\text{cm}^{-1}$, respectively. At the same time, the alkalinity test kits and hardness kits from Merck MERCK, Germany, were used to determine concentration values of HCO_3^- and Ca^{2+} , carried out with an error of 0.1 $\text{mmol}\cdot\text{L}^{-1}$ and 2 $\text{mg}\cdot\text{L}^{-1}$, respectively. Anions and cations were analyzed using an ICS-600 (TLYC/YQ-034) ion chromatograph from Thermo Fisher Instruments Inc. in the USA, and $\delta^{13}\text{C}_{\text{DIC}}$ isotopes were analyzed using a Delta V Advantage stable isotope mass spectrometer from Thermo Fisher Scientific Inc. in the USA, with a precision of 0.10‰~0.15‰. The anions, cations, and isotopes were all delivered to a lab for analytical testing. Among them, anions and cations were sent to Guizhou Tianlan Yunchuang Testing Co., Ltd. for testing, and isotopes were sent to the Third Institute of Oceanography of the Ministry of Natural Resources of China for testing.

Calculation Methods

$\delta^{13}\text{C}_{\text{DIC}}$ was calculated according to its formula [17]:

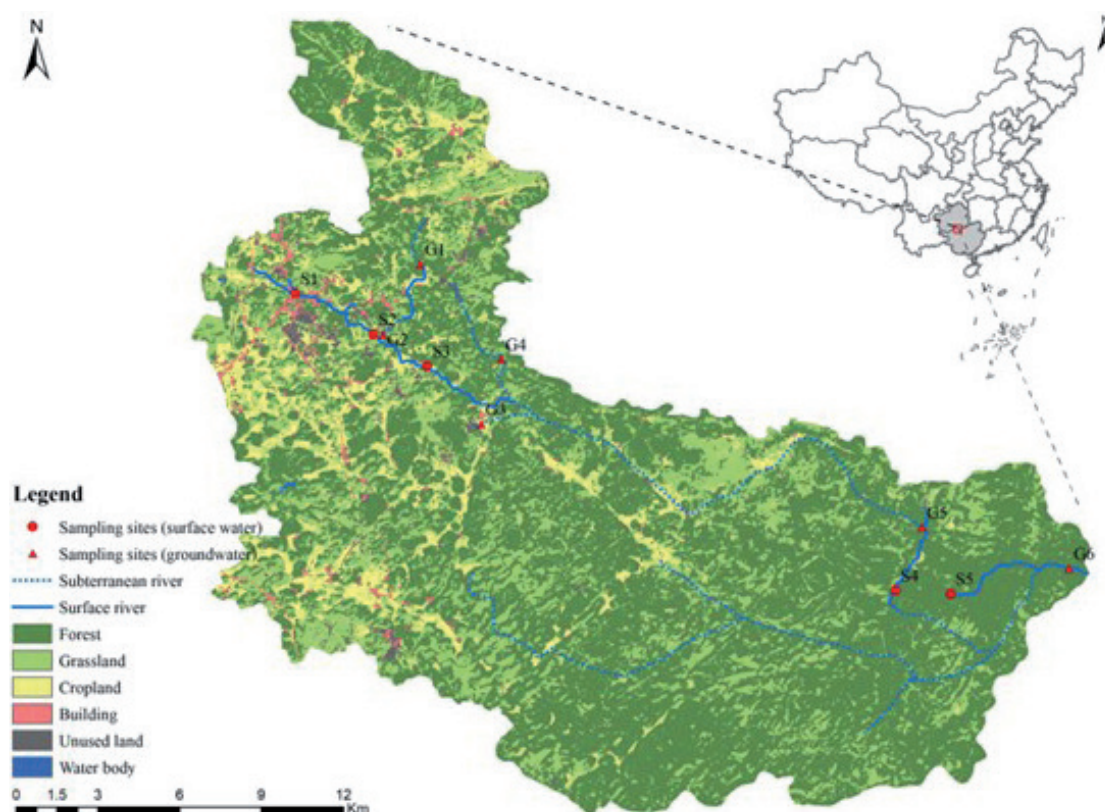


Fig. 1. Distribution of water sampling sites in the Huanghou underground river basin.

Table 1. Characteristics of the sampling points.



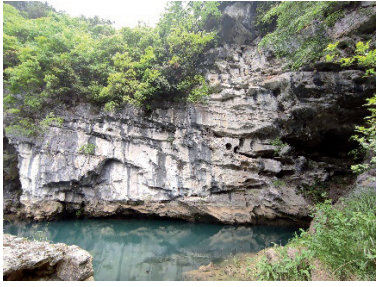




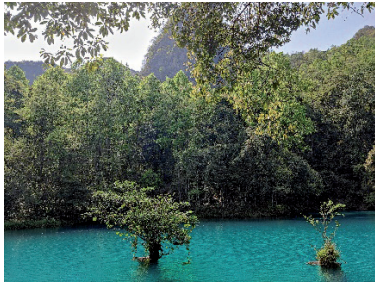
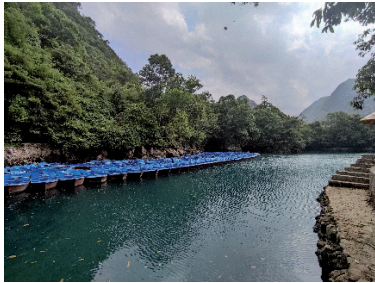

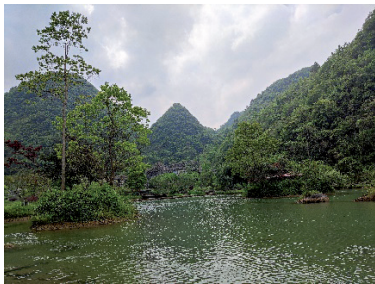
Sampling points	Photographs of the sampling points	Character analysis
S1		Located in a residential area of the town to which sewage from human activities may be discharged directly, the water is turbid and odorous.
S2		There is a sewage treatment plant within 10 meters of the site, which is surrounded by paddy fields planted with rice and oilseed rape.
G1		Located within the National Natural Water Resource Conservation Area, it is less affected by human activities.
G2		It is groundwater, surrounded by agricultural cultivation areas and generally low in anthropogenic activities other than agricultural activities.
S3		Located in Yaonan village, there is domestic waste discarded near the water column, the water column has an odour and cash crops are planted around it.
G3		The pool is a groundwater pumping and storage for Huanghou Dong, which is surrounded by arable land with more frequent agricultural activities.

Table 1. Table continued.

G4		It is groundwater, and the water extraction point at the bottom of the cave is more than 10 metres above the surface, which is usually not affected by human activities.
G4		Located in the lower reach of the river basin in a natural protected area with better environment.
S4		Located in the lower reach of the river basin in a natural protected area with better environment.
G6		Located in the lower reach of the river basin in a natural protected area. It is groundwater and generally less affected by visitors.
S5		Located in the lower reach of the river basin in a natural protected area with better environment.

$$\delta^{13}C_{DIC} = \left[\left(\frac{R_{sample}}{R_{VPDB}} - 1 \right) \times 1000 \right]$$

Where: R_{sample} represents the measured value of the sample and R_{VPDB} represents the standard sample value of 0.0112372. The calcite saturation index is widely used as an important indicator reflecting the dissolution

capacity of water bodies in the study of karst water columns [18]. Based on the measured physicochemical parameters such as each anion and cation, pH and water temperature, the calcite saturation index and the partial pressure of dissolved carbon dioxide (pCO_2) of the watershed water bodies were calculated using the PHREEQC-program [19]. The formulae are given below:

$$pCO_2 = [H^+][HCO_3^-]/(K_{CO_2} * K_1)$$

Where K_{CO_2} is the solubility coefficient of CO_2 and K_1 is the first dissociation constant for CO_2 dissolved in water. Calcite saturation index (SIc) was calculated as [20]:

$$SI_c = \log[(IAP)/(K_{SP})]$$

Where: IAP is the solubility product of each ion in calcite solution, and K_{SP} is the solubility product of calcite. When the calculation result meets $IAP > K_{SP}$ and $SIc > 0$, it means that calcite reaches saturation state and precipitation will occur; when it meets $IAP < K_{SP}$ and $SIc < 0$, it means that calcite is not saturated and dissolution of the mineral occurs.

Results and Discussion

Underground River Water Chemistry Characteristics

The water chemistry data of the watershed water bodies in the two seasons were analyzed, and the results are shown in Table 2. The range of water temperature variation in the dry season was from 12.50°C to 17.18°C, with a mean value of 15.00°C, and that in the rainy season was from 18.91°C to 20.03°C, with a mean value of 18.82°C. pH fluctuated from 7.48 to 8.64, with a mean value of 8.07, and the range of pH variations in the two seasons was close to each other. The watershed as a whole was weakly alkaline. DO, as a product of photosynthetic respiration and water-gas exchange of organisms, is usually used to reflect the strength of aquatic organisms' metabolism in the watershed based on its concentration [21], in which the highest DO value of 10.52 mg·L⁻¹ was observed at S2 in the dry season and the rainy season showed a gradual incremental increase, and the DO in the dry season was higher than that in the rainy season, which indicated that aquatic organisms metabolism was stronger in the dry season than that in the rainy season. The maximum values of conductivity in both seasons appeared in the S2 sample point, which was 388.20 μs·cm⁻¹ and 429.70 μs·cm⁻¹, respectively, compared to which, the conductivity of the groundwater sample point G6 in the scenic area was low. EC reflects the ionic strength of the water, and the trends of the conductivity changes were similar in both seasons, with the overall downstream conductivity being weaker than the upstream one, which may be caused by the gradual dilution effect from upstream to downstream with the flow of the water column. The EC values are significantly larger in the two sample points S1 and S2, which are likely to be related to the input of domestic sewage from the surrounding area.

River monitoring data showed that Ca^{2+} and Mg^{2+} dominated 98% of the cation. HCO_3^- accounted for

95% of the overall anions, and SO_4^{2-} accounted for 3%. HCO_3^- varied from 213.57 mg·L⁻¹ to 231.88 mg·L⁻¹ with a mean value of 221.34 mg·L⁻¹ in the dry season and 189.16 mg·L⁻¹ to 237.98 mg·L⁻¹ with a mean value of 206.36 mg·L⁻¹ in the rainy season. This is in line with the pH range of 7 to 9, as described by Liu et al. This is in agreement with Liu et al., who described that HCO_3^- occupies about 95% of the water column when the pH is between the range of 7 and 9 [22].

According to the water chemistry data of the two seasons, the measured abundance of cations in descending order was Na^+ (about 1%) < K^+ (1%) < Mg^{2+} (5%) < Ca^{2+} (93%), and Wei Xiaomei, in her study of the underground river basin of Mao Village, Guilin, showed that K^+ was more easily adsorbed and fixed in the groundwater than Na^+ , but the conclusion that the Na^+ concentration was lower than the K^+ concentration was made in the paper, and the reason for this was deduced to be the influence of human activities that slightly increased the K^+ concentration [23]. The relatively high values of K^+ concentration appeared in the two sample points S3 and G4 in the dry season and S2 in the rainy season, of which S3 is surrounded by an agricultural products planting area, and domestic rubbish can be seen discarded near the sampling point, and S2 is located 10 meters away from the wastewater treatment plant, and the increase in water flow in the rainy season will have an impact. The measured abundance of anions in order from smallest to largest are Cl^- (about 1%) < NO_3^- (1%) < SO_4^{2-} (3%) < HCO_3^- (95%); Cl^- is not involved in the chemical weathering reaction of rocks, and it is generally imported through the channels of agricultural activities such as the application of fertilizers containing potash salts and animal feces [24-25], and its lower content of Cl^- . Its low Cl^- concentration indicates that human activities do not have a significant impact on the water quality. The degree of influence of human activities on water quality was not obvious. During the rainy season, NO_3^- reached a maximum value of 12.80 mg·L⁻¹ at point S2, high likelihood of being affected by sewage treatment plant discharges. The subabundant anionic SO_4^{2-} in the watershed showed the highest values in the dry season at G2 (7.02 mg·L⁻¹) and G6 (7.74 mg·L⁻¹), where the G2 sampling site was surrounded by farmland and would be affected by agricultural activities, but its effect was small, while the rainy season showed a significant increase in the concentration of SO_4^{2-} at S1 (9.26 mg·L⁻¹), G5 (11.20 mg·L⁻¹) and S5 (9.26 mg·L⁻¹), the SO_4^{2-} concentrations significantly exceeded those in the dry season. Compared with the annual mean values of the concentrations determined by Zeng et al. for the water bodies in the Huanghou underground river basin during the five-year period from 2008 to 2012, Ca^{2+} (68.86 mg·L⁻¹-75.77 mg·L⁻¹), HCO_3^- (182.71 mg·L⁻¹-213.5 mg·L⁻¹) all showed a significant increase [26], and the rest of the concentrations decreased, with SO_4^{2-} decreasing up to 44%. However, for both the rainy and dry seasons, the mean ion concentration varies less and is mostly a background value for rock dissolution [27].

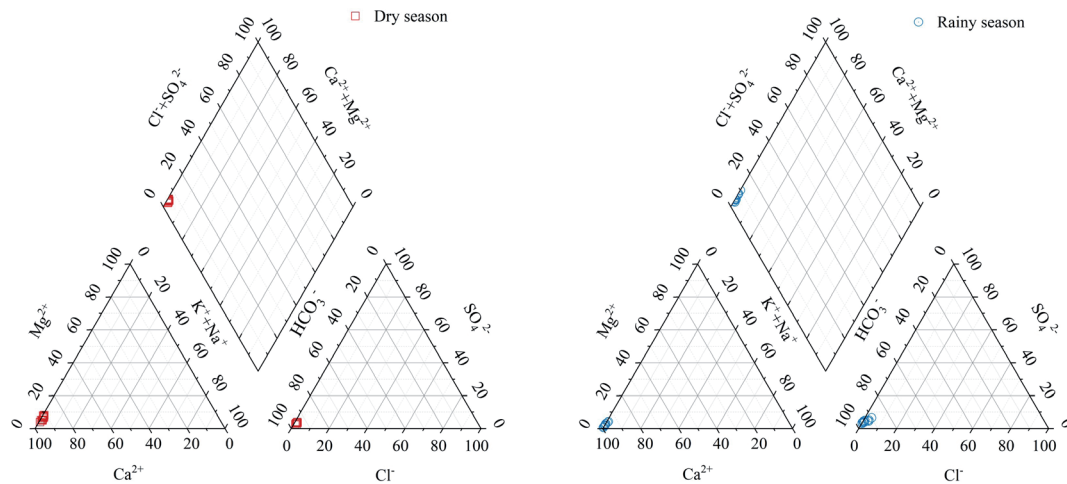


Fig. 2. Water chemistry piper diagram of the Huanghou River basin.

According to the following Piper diagram (Fig. 2), it can be clearly seen that the cations in the sampling points of the Huanghou underground river basin are significantly concentrated in the Ca^{2+} end, and the anions are significantly concentrated in the HCO_3^- end, thus judging that the hydrochemical type of the study area is HCO_3^- -Ca type, which is in line with the type of the water column judged by the previous researchers in this basin [26]. From Table 2, the measured water column ions $\text{Na}^+ / [\text{Na}^+ + \text{Ca}^{2+}]$ and $\text{Cl}^- / [\text{Cl}^- + \text{HCO}_3^-]$ ratios in the watershed were within 0.5 (Fig. 3). It is clear that the data distribution of the sampling points is within the range of rock weathering, which indicated that the study area was mainly affected by the weathering of rocks.

Seasonal Characteristics of DIC, $\delta^{13}\text{C}_{\text{DIC}}$, pCO_2 , and SIc

Dissolved inorganic carbon (DIC) is mainly carbonic acid (H_2CO_3), dissolved CO_2 , bicarbonate (HCO_3^-), and carbonate ions (CO_3^{2-}), and when the equilibrium state of the concentration of each of these components in the water column is mainly correlated with the temperature of the water, pH, and the strength of the ions therein, the pH range of 7-9 is mainly in the form of HCO_3^- . When the pH is weakly alkaline, it mainly exists in the form of HCO_3^- ; when the pH is lower, it mainly exists in the form of H_2CO_3 [28-29]. The pH dynamics in the Huanghou underground river basin are divided into the range of 7.48-8.64, in which the HCO_3^- value occupies 95% of the carbonate equilibrium system, and therefore the DIC is expressed in terms of the concentration of HCO_3^- [30].

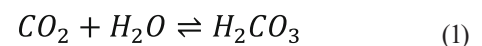
The dry season mean value of DIC concentration in the waters of the basin was $221.34 \text{ mg}\cdot\text{L}^{-1}$, and the rainy season mean value was $206.36 \text{ mg}\cdot\text{L}^{-1}$, with higher concentrations in the dry season compared to the rainy season. The decrease in DIC values may be due to the dilution effect of increased rainfall in the rainy season on the watershed, whereas the highest DIC values

were observed at the S2 sample point (Fig. 4a), which is near the wastewater treatment plant and surrounded by agricultural cultivation areas, and the washing of rainwater may cause a large amount of soil CO_2 to enter the water, which resulted in the increase of the DIC concentration. The mean value of $\delta^{13}\text{C}_{\text{DIC}}$ was -4.91‰ in the dry season and -9.97‰ in the rainy season, and the $\delta^{13}\text{C}_{\text{DIC}}$ of the watershed water was significantly more positive in the dry season than that in the rainy season. For the calcite saturation index, the spatial fluctuations were similar, the SIc values were all > 0 , and the water bodies were all in a slightly oversaturated state. pCO_2 values varied in the range of the dry season to show that the partial pressure in the rainy season was higher than that in the dry season, which showed obvious seasonal variations.

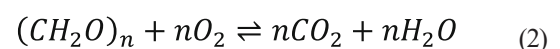
Exploration of the Sources of DIC in Watersheds

The sources of DIC in karst water bodies include three main aspects: dissolution of carbonate rocks, atmospheric CO_2 , and oxidative decomposition of soil organic matter [31-32]. Different DIC sources have differentiated $\delta^{13}\text{C}_{\text{DIC}}$ values, so $\delta^{13}\text{C}_{\text{DIC}}$ is an important indicator of the source of DIC in water bodies. The formation of DIC in water bodies with the involvement of various mechanisms is shown in the following equation [33]:

CO_2 dissolution reaction processes (in soil vs. air):



Oxidative decomposition of organic matter:



Weathering of carbonate rocks (carbonate, sulfate, nitrate):

Table 2. Data table of the measured water chemistry concentrations in the Huanghou underground river basin.

Time	Sampling points	Temperature °C	pH	EC μs/cm	DO	K ⁺	Ca ²⁺	Na ⁺	Mg ²⁺	Cl ⁻	NO ₃ ⁻	SO ₄ ²⁻	HCO ₃ ⁻	NICB %	Na ⁺ /(Na ⁺ +Ca ²⁺) Concentration ratio	Cl ⁻ /(Cl ⁻ +HCO ₃ ⁻)
February	S1	12.51	8.08	372.70	8.52	0.42	86.00	0.95	3.54	1.34	2.26	6.59	231.88	13.53	0.011	0.006
	S2	13.78	8.57	388.20	10.52	0.00	86.00	0.94	4.19	1.71	0.00	6.43	225.77	17.08	0.011	0.008
	G1	13.17	8.42	312.30	9.07	0.39	76.00	0.10	3.92	1.37	2.33	5.89	213.57	10.52	0.001	0.006
	G2	13.90	8.37	314.00	9.84	0.31	74.00	0.56	3.95	1.65	0.96	7.02	219.67	6.06	0.008	0.007
	S3	13.06	8.42	345.20	9.39	1.16	80.00	0.62	3.57	1.95	1.79	6.63	219.67	12.06	0.008	0.009
	G3	14.49	8.15	348.60	8.56	1.22	82.00	0.04	3.79	2.31	1.56	6.85	231.88	9.18	0.001	0.010
	G4	17.10	8.14	307.30	7.60	0.30	68.00	1.00	2.16	2.31	2.99	4.33	219.67	-4.95	0.015	0.010
	G5	17.16	8.17	326.20	7.83	0.89	73.00	0.63	2.56	1.19	1.21	4.49	213.57	6.63	0.009	0.006
	S4	16.13	8.64	321.30	8.25	0.75	80.00	0.18	1.98	1.35	1.04	5.56	213.57	12.28	0.002	0.006
	G6	17.18	8.40	296.30	9.03	0.64	84.00	0.15	2.74	1.72	1.91	7.74	231.88	9.07	0.002	0.007
May	S5	16.51	8.61	301.50	9.05	0.66	74.00	0.55	2.42	1.61	0.81	5.68	213.57	6.57	0.007	0.007
	S1	18.91	7.57	386.00	5.85	0.00	74.00	0.25	0.27	0.99	1.44	9.26	219.67	-3.17	0.003	0.004
	S2	20.03	7.74	429.70	7.20	1.08	84.00	0.26	2.27	0.00	12.80	6.95	237.98	3.81	0.003	0.000
	G1	17.80	7.74	324.40	7.94	0.00	72.00	0.24	0.27	1.24	0.42	6.41	201.37	4.16	0.003	0.006
	G2	20.03	7.84	320.10	7.82	0.90	68.00	1.39	1.63	0.39	6.48	7.54	195.26	3.86	0.020	0.002
	S3	18.98	7.74	378.70	8.00	0.25	74.00	1.24	0.96	0.59	5.01	7.16	219.67	-0.35	0.016	0.003
	G3	19.65	7.50	356.00	7.78	0.27	76.00	0.11	1.00	0.56	2.15	7.37	213.57	4.71	0.001	0.003
	G4	17.26	7.48	351.60	7.71	0.17	72.00	0.11	1.35	0.36	3.96	4.85	189.16	11.81	0.002	0.002
	G5	18.16	7.65	335.90	8.30	0.22	68.00	0.02	0.70	4.46	4.02	11.20	195.26	-4.77	0.000	0.022
	S4	19.17	7.91	333.30	8.79	0.22	72.00	0.15	0.86	3.63	2.85	7.34	189.16	7.51	0.002	0.019
	G6	18.46	8.19	319.70	9.55	0.06	70.00	0.17	0.42	2.81	1.82	8.28	201.37	-1.22	0.003	0.014
	S5	18.58	8.25	319.10	9.69	0.24	74.00	0.05	1.27	3.61	2.89	9.36	207.47	1.66	0.000	0.017

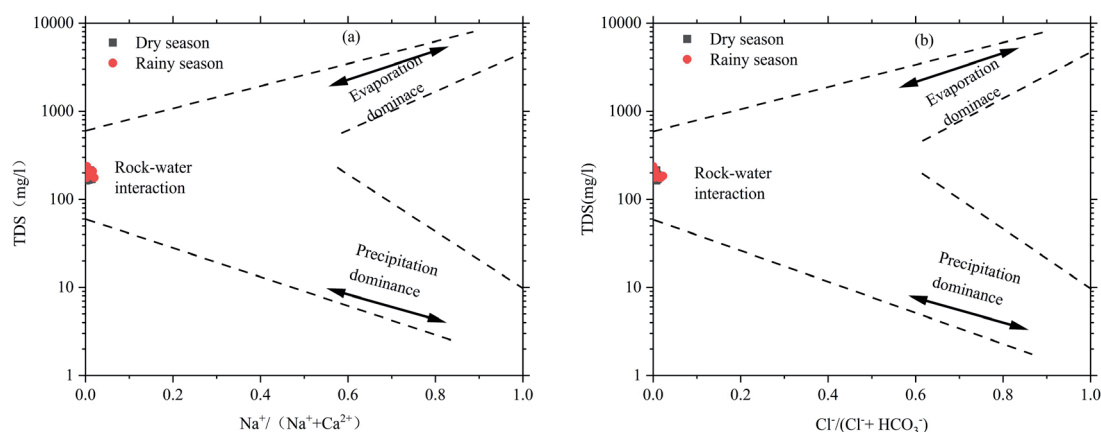
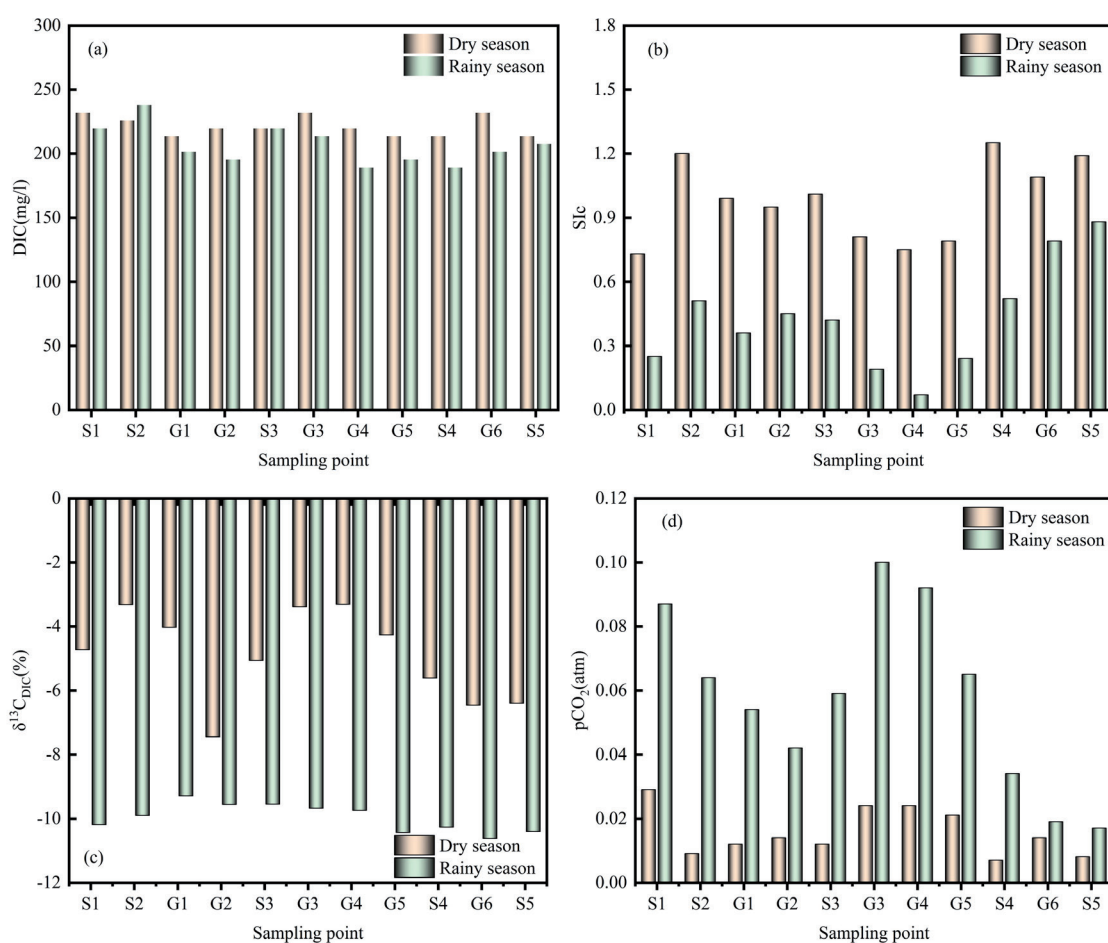
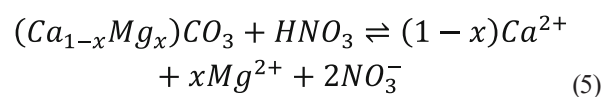
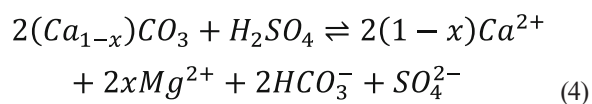
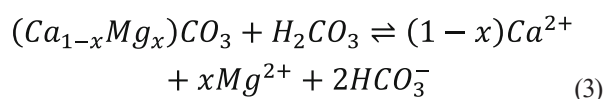


Fig. 3. Gibbs plot of water chemistry in the Huanghou River Basin.


 Fig. 4. Seasonal variation of DIC, SIc, $\delta^{13}\text{CDIC}$ and pCO_2 in the watershed waters.


The dissolution rate of carbonate rock in karst areas is fast, and the pCO_2 of the watershed water column is much higher than that of the atmosphere, so the percentage of atmospheric CO_2 is not considered when judging the source of DIC [4]. From the measured data

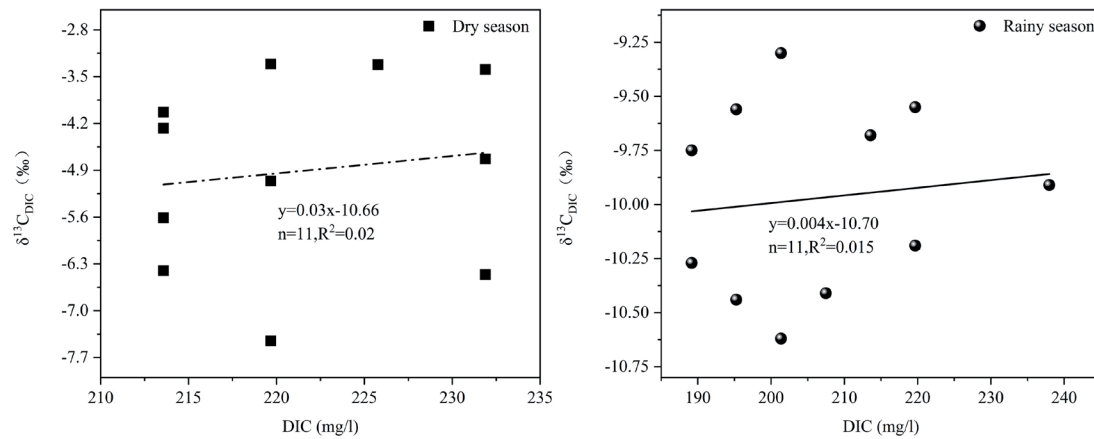


Fig. 5. Correlation analysis of DIC and $\delta^{13}\text{C}_{\text{DIC}}$ plotted.

of water chemistry in the Huanghou underground river basin in Table 2, the range of $\delta^{13}\text{C}_{\text{DIC}}$ changes in the dry season is $-7.45\text{‰} \sim -3.31\text{‰}$, which is not a significant difference from that of the bare-rock land (average of -3.03‰) [34], suggesting that the source of DIC in the dry season is mainly the dissolution of carbonate rock; in the rainy season, the variation ranged from -10.62‰ to -9.30‰ , with a mean value of -9.97‰ . The significantly high $\delta^{13}\text{C}_{\text{DIC}}$ in the dry season, combined with the fact that all the above water bodies had $\text{SIc} > 0$ and pCO_2 above atmospheric pressure, inferred that degassing was occurring, hence the positive $\delta^{13}\text{C}_{\text{DIC}}$ results [35]. However, as shown in Fig. 4(b) (c), the trend similarity between SIc and $\delta^{13}\text{C}_{\text{DIC}}$ fluctuations is not strong, indicating that degassing is present but not significant [19]. For the study of dissolved inorganic carbon (DIC) and its isotopes in karst groundwater systems, Cane, Li, and Li et al. explored and analyzed karst groundwater in the Raisin River area in Canada and groundwater in the Guiyang area and karst groundwater in the Shuicheng Basin, respectively, and found that no correlation exists between DIC and $\delta^{13}\text{C}_{\text{DIC}}$ [25, 36-37], and the results of this study indicate that the influencing factors of $\delta^{13}\text{C}_{\text{DIC}}$ do not have a unitary. As shown in the following figure (Fig. 5), the correlation analysis between DIC and $\delta^{13}\text{C}_{\text{DIC}}$ in the dry and rainy seasons in this study area showed a poor correlation, and it can be concluded that the source of DIC in the study area is not only the dissolution of carbonate rocks, but also the participation of external factors. The main sources of DIC in the study area are carbonate weathering and soil CO_2 .

The quantitative resolution of DIC sources is estimated using an isotopic mass balance model with the following equation [9]:

$$\delta^{13}\text{C}_{\text{DIC}} = X \times \delta^{13}\text{C}_A + (1 - X)\delta^{13}\text{C}_B \quad (6)$$

Where: $\delta^{13}\text{C}_A$ represents the $\delta^{13}\text{C}$ value of the carbonate carbon pool, $\delta^{13}\text{C}_B$ represents the $\delta^{13}\text{C}$ value of the soil carbon pool, and X represents the contribution ratio of the carbonate carbon pool to the $\delta^{13}\text{C}_{\text{DIC}}$ of the

water body. Because the rock layers in the study area belong to marine carbonate rocks, its $\delta^{13}\text{C}$ is generally 0‰ . Studies have shown that the $\delta^{13}\text{C}$ value of CO_2 in soils in the karst region of Guizhou is about -23‰ [20]. Based on Eq. (6), it was calculated that 86.52% to 67.61% of the dry season DIC was derived from dissolved carbonate rocks and 13.48% to 32.39% from soil CO_2 , while 59.57% to 53.83% of the rainy season DIC was derived from dissolved carbonate rocks and 40.43% to 46.17% from soil CO_2 .

Analysis of Factors Influencing Seasonal Changes in DIC

Liu Zaihua et al. showed that the dynamics of groundwater HCO_3^- is closely related to the dynamics of soil CO_2 and the dynamics of rainfall and that the content of soil CO_2 increases with increasing temperature and is more favorable to the dissolution of carbonate, which leads to an increase in the concentration of DIC in the water column [38]. Hydrological conditions in river systems are an important control of carbon synthesis and decomposition in rivers [39]. Water temperature and rainfall levels in a river basin affect carbon synthesis and decomposition in rivers, as well as the respiration of plants, decomposition of organic matter, and soil moisture in the watershed, resulting in a differentiated distribution of carbon concentrations in rivers in different seasons [40-41]. The analysis of the along-range variation of DIC in the watershed on the spatial and temporal scales showed that in the temporal distribution range, the mean value of DIC concentration in the dry season was $221.34 \text{ mg}\cdot\text{L}^{-1}$, with the maximum value ($231.88 \text{ mg}\cdot\text{L}^{-1}$) reached simultaneously at G1, W3, and W6, and the maximum value of $237.98 \text{ mg}\cdot\text{L}^{-1}$ was reached at G2 in the two months. It was inferred that the elevated DIC at this sampling point was related to the discharge from the wastewater treatment plant. The average value of DIC concentration in the rainy season was $206.36 \text{ mg}\cdot\text{L}^{-1}$, which was significantly lower than that in the dry season, and its spatial variation fluctuated greatly, which was analyzed to be the possible reason for

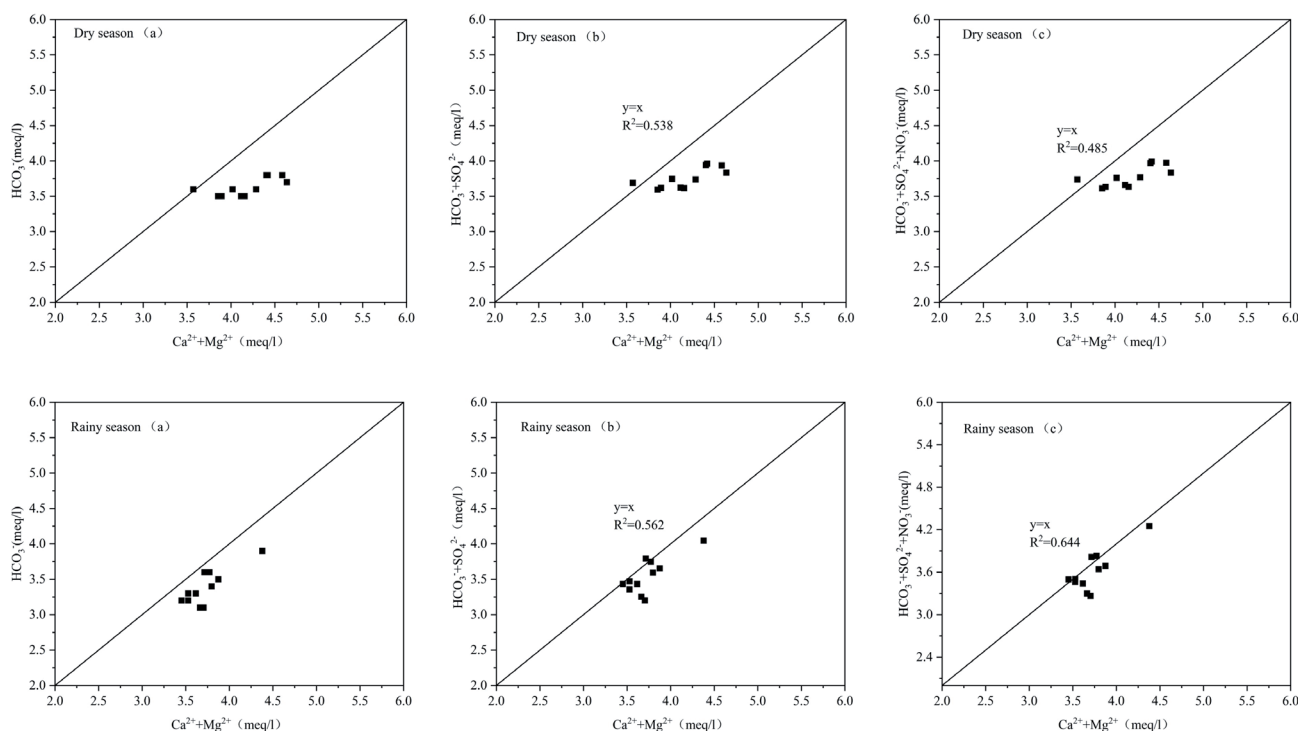


Fig. 6. Anion-cation relationship in water.

the decrease in the river level in the dry season, thus, the interaction between surface water and groundwater was further enhanced [42], and the recharge of groundwater to the surface water would correspondingly increase the concentration of DIC in the dry season. In addition, the increase in river level during the rainy season dilutes the DIC concentration in the watershed to a certain extent, and coupled with the accelerated flow rate of the river, it reduces the time of rock-water reaction and lowers the concentration of DIC in the rainy season [18].

Analysis of Factors Influencing Seasonal Changes in $\delta^{13}\text{C}_{\text{DIC}}$

For $\delta^{13}\text{C}_{\text{DIC}}$ values, the $\delta^{13}\text{C}_{\text{DIC}}$ of the basin as a whole highlighted significant seasonal differences. The $\delta^{13}\text{C}_{\text{DIC}}$ in the basin was in a smooth drive in the rainy season and was the lightest in the four sampling points at the headwaters and downstream, which were -10.19‰, -10.44‰, -10.27‰, -10.62‰, and -10.41‰, respectively, and the $\delta^{13}\text{C}_{\text{DIC}}$ in the rainy season as a whole was more impoverished than that in the dry season (i.e., the $\delta^{13}\text{C}_{\text{DIC}}$ values were more negative). Liu and Zhao et al. in their studies of Banzhai, Chenqi, and Dengzhang River also concluded that the $\delta^{13}\text{C}_{\text{DIC}}$ in the rainy season was lighter than that in the dry season [8, 43]. This is attributed to the higher temperatures and humidity during the rainy season, the increased activity of organisms in the water, the significant decomposition of organic matter by soil microorganisms, and the washout of rainwater that results in more abundant soil CO_2 entering the water column, thus making the $\delta^{13}\text{C}_{\text{DIC}}$ values overall more

negative during the rainy season [44]. The $\delta^{13}\text{C}_{\text{DIC}}$ values in the dry season show the lightest state throughout the season in W2 and then show the fluctuation of first heavier and then lighter. The slowing down of the river flow rate in the dry season can make the phytoplankton in the surface water absorb lighter DIC isotopes in the water column, and thus the isotopes in the river water are relatively enriched [45]. At the same time, soil respiration produces less CO_2 , carbonate dissolution is low, and groundwater has high $\delta^{13}\text{C}_{\text{DIC}}$ values and low pCO_2 [34]. In addition, the involvement of exogenous acids (e.g., sulfuric acid, nitric acid, etc.) can also lead to positive $\delta^{13}\text{C}_{\text{DIC}}$ values in water bodies.

The study shows that the $(\text{Ca}^{2+}+\text{Mg}^{2+})$ to (HCO_3^-) equivalence ratio for areas controlled by carbonate rock weathering should satisfy a linear relationship of $y=x$ [20], while by Fig. 6a (dry season and rainy season), the linear condition is not satisfied, then there should be anions in addition to HCO_3^- to make up for the 1:1 relationship. Figs. 6b (dry season) and 6bc (rainy season) show that in the presence of SO_4^{2-} and NO_3^- , the equivalence ratios of the ions show a good correlation, suggesting that sulfuric acid and nitric acid are involved in the weathering process of carbonate rocks, where the significance of the involvement of exogenous acids in the weathering of rocks is slightly stronger in the rainy season than that in the dry season.

Conclusions

In this paper, the following conclusions were drawn by analyzing the characteristics of water chemistry, DIC, and its isotopic variations in different seasonal periods in the Huanghou Underground River Basin, as well as exploring the sources and seasonal variation factors of DIC and $\delta^{13}\text{C}_{\text{DIC}}$:

(1) According to Piper's trilinear diagram, the chemical type of the water in the Huanghou underground river basin is $\text{HCO}_3\text{-Ca}$ type, and the ions in the water are Ca^{2+} and HCO_3^- as the main cations and anions, both of which occupy 98% of the overall cation and anion concentration, respectively, and the concentration and source of the ions indicate that the anthropogenic activities have caused a relatively small impact on the water in the study area.

(2) Both DIC and $\delta^{13}\text{C}_{\text{DIC}}$ in the basin showed obvious seasonal variations, with DIC being higher in the dry season than that in the rainy season, suggesting a stronger dilution of the water and a decrease in the rock-water reaction time in the rainy season. The soil in the dry season is drier and at lower temperatures, with less CO_2 produced by its respiration, degassing, and nitric and sulfuric acids involved in the weathering of the rock, making the $\delta^{13}\text{C}_{\text{DIC}}$ value significantly positive compared with the rainy season.

(3) The sources of DIC in the water bodies of the study area are mainly the dissolution of carbonate rocks and soil CO_2 , with less influence from external involvement. The source of DIC in the dry season ranged from 86.52% to 67.61% from dissolved carbonate rocks and from 13.48% to 32.39% from soil CO_2 , while the source of DIC in the rainy season ranged from 59.57% to 53.83% from dissolved carbonate rocks and from 40.43% to 46.17% from soil CO_2 .

Acknowledgments

The Authors wish to thank all the researchers of the paper for their supporting, and Guizhou Provincial Key Technology R&D Program: A study on the conservation model with technology and sustainable development demonstration of the World Natural Heritages in Guizhou (No. 220 2023 QKHZC) and the China Overseas Expertise Introduction Project for Discipline Innovation (China 111 Project) [grant number: D17016] for financial support.

Conflict of Interest

The authors declare no conflict of interest.

References

1. SUN H.G., HAN J.T., LI D.W., LU X.X., ZHANG H.B., ZHAO W. Organic carbon transport in the Songhua River, NE China: Influence of land use. *Hydrological Processes*, **31** (11), 2062, **2017**.
2. KWON E.Y., DEVRIES T., GALBRAITH E.D., HWANG J., KIM, G., TIMMERMANN A. Stable Carbon Isotopes Suggest Large Terrestrial Carbon Inputs to the Global Ocean. *Global Biogeochemical Cycles*, **35** (04), 25, **2021**.
3. CHAPLOT V., MUTEMA M. Sources and main controls of dissolved organic and inorganic carbon in river basins: A worldwide meta-analysis. *Journal of Hydrology*, **603**, 126941, **2021**.
4. LIU J., ZHONG J., DING H., YUE F., LI C., XU S., LI S. L. Hydrological regulation of chemical weathering and dissolved inorganic carbon biogeochemical processes in a monsoonal river. *Hydrological Processes*, **34**, 2780, **2020** [In Chinese].
5. GE T.T., LUO C., REN P., ZHANG H.M., FAN D., CHEN H.T., CHEN Z.H., ZHANG J., WANG X.C. Stable carbon isotopes of dissolved inorganic carbon in the Western North Pacific Ocean: Proxy for water mixing and dynamics. *Frontiers in Marine Science*, **9**, 13, **2022**.
6. NOWAK M.E., SCHWAB V.F., LAZAR C.S., BEHRENDT T., KOHLHEPP B., TOTSCH K.U., KÜSEL K., TRUMBORE S.E. Carbon isotopes of dissolved inorganic carbon reflect utilization of different carbon sources by microbial communities in two limestone aquifer assemblages. *Hydrology and Earth System Sciences*, **21** (09), 4283, **2017**.
7. QIBO H., XIAOQUN Q., PENGYU L., LIANKAI Z., RUIRUI C., TENG FANG L.I. Characteristics and control factors of dissolved inorganic carbon in karst groundwater in Liuling Spring catchment, Lüliang, Shanxi. *Geological Review*, **65** (04), 961, **2019** [In Chinese].
8. MIN Z., CENG Z., ZAIHUA L. Influence of land use change on dissolved inorganic carbon and stable isotopic compositions of karst groundwater. *Geochimica*, **38** (06), 565, **2009**.
9. YI Z., SHENGZHANG Z.O.U., HAOYONG S., FUNING L.A.N., HAO X.I.E., JUN L.I. Source and control factors of main ions and dissolved inorganic carbon in the lakes of Huixian Karst Wetland. *Geology In China*, **2024** [In Chinese].
10. ZHANG C., XIAO Q. Study on dissolved inorganic carbon migration and aquatic photosynthesis sequestration in Lijiang River, Guilin. *Carsologica Sinica*, **40** (04), 555, **2021** [In Chinese].
11. QIN C.Q., LI S.L., YUE F.J., XU S., DING H. Spatiotemporal variations of dissolved inorganic carbon and controlling factors in a small karstic catchment, Southwestern China. *Earth Surface Processes and Landforms*, **44** (12), 2423, **2019**.
12. CALABRESE S., PORPORATO A., PAROLARI A.J. Hydrologic Transport of Dissolved Inorganic Carbon and Its Control on Chemical Weathering. *Journal of Geophysical Research-Earth Surface*, **122** (10), **2017**.
13. XIE Y., HUANG F., YANG H., YU S. Role of anthropogenic sulfuric and nitric acids in carbonate weathering and associated carbon sink budget in a karst catchment (Guohua), southwestern China. *Journal of Hydrology*, **599**, 126287, **2021**.
14. MAO J.Q., LI J.Y. Karst Development Controlled by Structure Network in South Dushan, Guizhou Province. *Geographical Research*, **5** (04), 47, **1986** [In Chinese].
15. LUKAČ REBERSKI J., TERZIĆ J., MAURICE L., LAPWORTH D.J. Emerging organic contaminants in karst groundwater: A global level assessment. *Journal of Hydrology*, **2021**.

16. LI J.Y., JI C.M., YE G.Q., LIU K.X., LIANG F. Characteristics and Assessment On Water Resources of Huanghou Karst Underground Drainage at Dushan In South Guizhou Province. *Carsologica Sinica*, **18** (03), 39, **1999**.
17. RAMON A., SCHIFF S.L., TRUMBORE S.E., DILLON P.J., RICHARD E. Evaluating Dissolved Inorganic Carbon Cycling in a Forested Lake Watershed Using Carbon Isotopes. *Radiocarbon*, **34** (03), 636, **2016**.
18. LI C., ZHANG X., GAO X., LI C., JIANG C., LIU W., LIN G., ZHANG X., FANG J., MA L. Spatial and temporal evolution of groundwater chemistry of baotu karst water system at northern China. *Minerals*, **12** (3), 348, **2022**.
19. LUO J., LI S., NI M., ZHANG J. Large spatiotemporal shifts of CO₂ partial pressure and CO₂ degassing in a monsoonal headwater stream. *Journal of Hydrology*, **579**, 124135, **2019**.
20. DING S.J., ZHOU Z.F., XUE B.G., TANG Y.T., ZHU C.C., AN D., FAN B.X. Analysis of Hydrochemistry and $\delta^{13}\text{C}_{\text{DIC}}$ Characteristics in the Weiyuan River of Southwest Karst Area. *Journal Of China Hydrology*, **40** (05), 78, **2020** [In Chinese].
21. DING S.J. Characteristics of Dissolved Inorganic Carbon in Karst Watersheds and the Mechanisms Influencing Carbon Fluxes at the Water-air Interface, **2022** [In Chinese].
22. LIU Z., DREYBRODT W., WANG H. A new direction in effective accounting for the atmospheric CO₂ budget: Considering the combined action of carbonate dissolution, the global water cycle and photosynthetic uptake of DIC by aquatic organisms. *Earth-Science Reviews*, **99**, 162, **2010**.
23. WEI X.M. Analysis of Hydrochemical Characteristics and Its Impact Factors of Maocun Underground River Basin in Guilin, Guangxi, **2021** [In Chinese].
24. SHERWOOD W.C. Chloride loading in the South Fork of the Shenandoah River, Virginia, U.S.A. *Environmental Geology*, **14** (02), 99, **1989**.
25. LI X.D., LIU C.Q., HARUE M., LI S.L., LIU X.L. The use of environmental isotopic (C, Sr, S) and hydrochemical tracers to characterize anthropogenic effects on karst groundwater quality: A case study of the Shuicheng Basin, SW China. *Applied Geochemistry*, **25** (12), 1924, **2010**.
26. ZENG C., LIU Z., ZHAO M., YANG R. Hydrologically-driven variations in the karst-related carbon sink fluxes: Insights from high-resolution monitoring of three karst catchments in Southwest China. *Journal of Hydrology*, **533**, 74, **2016**.
27. XINGHUI X., LITIAN Z., JINGSHENG C. The Effect of Lithology and Climate on Major Ion Chemistry of the Yangtze River System. *Acta Scientiarum Naturalium Universitatis Pekinesis*, **36** (02), 246, **2000**.
28. LIU J., ZHONG J., DING H., YUE F., LI C., XU S., LI S.L. Hydrological regulation of chemical weathering and dissolved inorganic carbon biogeochemical processes in a monsoonal river. *Hydrological Processes*, **34**, 2780, **2020**.
29. HAN X., CHENG X., LI S., YUAN J., ZHANG Q. Carbon concentrations and their stable isotopic signatures in the upper Han River, China. *Environmental Science and Pollution Research*, **26**, 14116, **2019**.
30. LIN J., SU Y.P., ZHONG H.Z., CHEN Y.Z., LI Y.F., LIN H. Vertical distribution of phytoplankton in a eutrophic reservoir, Shanzi Reservoir (fuian) during summer stratification. *Journal of Lake Sciences*, **22** (02), 244, **2010**.
31. ZHANG Y., JIANG Y., YUAN D., CUI J., LI Y., YANG J., CAO M. Source and flux of anthropogenically enhanced dissolved inorganic carbon: a comparative study of urban and forest karst catchments in Southwest China. *Science of the total environment*, **725**, 138255, **2020**.
32. BROWN K.A., MCLAUGHLIN F., TORTELL P.D., YAMAMOTO-KAWAI M., FRANCOIS R. Sources of dissolved inorganic carbon to the Canada Basin halocline: A multitracer study. *Journal of Geophysical Research: Oceans*, **121** (5), 2918, **2016**.
33. LI L., PU J.B., LI J.H., ZHANG T. Temporal and Spatial Variations of Dissolved Inorganic Carbon and Its Stable Isotopic Composition in the Surface Stream of Karst Groundwater Recharge. *Environmental Science*, **38** (02), 527, **2017**.
34. LI D., ZHAO M., LIU Z.H., CHEN B. Dual carbon isotope($\delta^{13}\text{C}$ - $\Delta^{14}\text{C}$) characteristics and carbon footprint in the spring-pond systems at the Puding Karst Water-Carbon Cycle Test site. *Earth Science Frontiers*, **29** (03), 155, **2022** (Chinese).
35. LI S.L., LIU C.Q., LI J., LANG Y.C., DING H., LI L. Geochemistry of dissolved inorganic carbon and carbonate weathering in a small typical karstic catchment of Southwest China: Isotopic and chemical constraints. *Chemical Geology*, **277** (3-4), 301, **2010**.
36. CANE G., CLARK I.D. Tracing Ground Water Recharge in an Agricultural Watershed with Isotopes. *Ground Water*, **37** (01), 133, **1999**.
37. LI S.L., LIU C.Q., LI J., LANG Y.C., DING H., LI L. Geochemistry of dissolved inorganic carbon and carbonate weathering in a small typical karstic catchment of Southwest China: Isotopic and chemical constraints. *Chemical Geology*, **277** (3-4), 301, **2010**.
38. LIU Z.H., YUAN D.X. Features of Geochemical Variations in Typical Epikarst Systems of China and Their Environmental Significance. *Geological Review*, **46** (03), 324, **2000** [In Chinese].
39. DING B.L., LI X.J., JIANG D.J. Research Progress on Carbon in River Waters. *Pearl River*, **41** (11), 37, **2020** (Chinese).
40. QIAO H.J. Influence of Agricultural Landscape on Riverine Dissolved organic Carbon Loading Rates during Storm Events, **2016** [In Chinese].
41. MA X.L., LIU G.M., WU X.D., XU H.Y., YE L.L., ZHANG X.L. Seasonal Variations of Dissolved Organic Carbon Exports in streams Under Alpine Meadow in the Three Rivers' Headwater Regions, Qinghai-Tibetan Plateau. *Resources and Environment in the Yangtze Basin*, **27** (10), 2387, **2018**.
42. JIANG D.J., LI Z., LUO Y.M., XIA Y. River Damming and Drought Affect Water Cycle Dynamics in an Ephemeral River Based on Stable Isotopes: The Dagui River of North China. *Science of The Total Environment*, **758**, 143682, **2020**.
43. LIU J., ZHONG J., CHEN S., XU S., LI S.L. Hydrological and biogeochemical controls on temporal variations of dissolved carbon and solutes in a karst river, South China. *Environmental Sciences Europe*, **33** (01), 1, **2021**.
44. LI Y.H., GE G., HU C.H. Sources, transportations and variation characteristics of dissolved inorganic carbon in Lake Poyang, China. *Journal of Lake Sciences*, **34** (2), 528, **2022**.
45. CAO X.X. Study on geochemical process of karst wetland basin based on changes of water chemistry and stable isotope, **2016** [In Chinese].